Optimal Design of Sustainable Power-to-Fuels Supply Chains for Seasonal Energy Storage

Antonio Sánchez[a], Mariano Martín[a], Qi Zhang[b,*]

[a]*Department of Chemical Engineering, University of Salamanca, 37008 Salamanca, Spain*
[b]*Department of Chemical Engineering and Materials Science, University of Minnesota, Minneapolis, MN 55455, USA*

Abstract

Energy storage is key in enabling high penetration of intermittent renewable sources into the energy supply mix. One attractive way of storing energy is to do so in the form of chemical fuels produced from electricity, also referred to as "power-to-fuels". Apart from its promise for large-scale seasonal energy storage, it also has advantages at the supply chain level due to the ease of transportation. Therefore, these fuels have been proposed as energy carriers for various applications. In this work, these potential benefits are assessed by optimizing the design of power-to-fuels supply chains for seasonal energy storage over large geographical regions. Distribution decisions are integrated with hourly production decisions over the time horizon of a year in order to account for seasonal changes and obtain plant capacities suitable for time-varying operation. A heuristic decomposition approach is developed to solve industrial-scale instances of the resulting optimization problem. The proposed framework is applied to a region of Spain where the energy transition is particularly significant due to the decommissioning of coal-based power generation facilities. The results show how an efficient power-to-fuels supply chain can help replace conventional with renewable energy sources.

Keywords: Power-to-fuels, Chemical energy storage, Power-to-X, Renewable energy

1. Introduction

The power, heat, and transportation sectors combined are responsible for about 65% of the global CO_2 emissions (Nejat et al., 2015). Due to sustainability concerns, the share of renewable energy has been increasing rapidly over the last few decades (Mehigan et al., 2020). In the heating and cooling sector, decarbonization is one of the main

*Corresponding author
Email address: qizh@umn.edu (Qi Zhang)

targets to achieve climate neutrality, and, at this point, the integration of electricity and heat is crucial (Thomaßen et al., 2021). In addition, in a renewable energy scheme, a transition is required in the transportation sector. Electrification of some applications such as small vehicles combined with the use of different renewable fuels for large energy consumption such as maritime or air transport has been proposed (García-Olivares et al., 2018). In all cases, power production using renewable sources is the core activity in the new renewable energy system. According to recent predictions (BloombergNEF, 2019), in 2050, 62% of the power will be produced from renewable sources and 48% of the power generation will come from solar and wind. The main challenge in the use of these two resources is the strong weather dependence (Alves et al., 2020). The sudden and large fluctuations in wind and solar availability lead to large changes in the power output from, for example, PV panels and wind turbines, in contrast to traditional energy sources (Leonard et al., 2018). Consequently, this fact determines the operation of the energy system and its stability may be jeopardized with an increase in the penetration of renewable energy sources. To deal with this challenge, a combination of intermittent and non-intermittent renewable sources along with energy storage will be required (Heuberger et al., 2017).

In this context, a wide range of energy storage technologies are being considered (Ajanovic et al., 2020) with different environmental impacts (Sternberg and Bardow, 2015). According to Gür (2018), there are four main categories of storage: mechanical, chemical, electrochemical and electrical. The different alternatives are characterized, mainly, by their power ratings and discharge times. Only two of these options are available at commercial scale now: pumped-hydro and compressed-air energy storage (CAES). Pumped-hydro can deal with a large range of storage timescales; however, there is little room for expanding the current capacity (Larsen and Petersen, 2013). CAES is an interesting option for large-scale power storage, but has only found limited application due to its relatively low energy density and the need for suitable geological caverns (Bartela, 2020).

Producing chemical fuels from electricity and using them as energy storage has attracted much attention due to the high energy density of these chemicals, the scalable and flexible behavior of this technology and ease of storage and transportation (Burre et al., 2020). Different fuels that have been proposed are hydrogen (Zhang et al., 2019b), methane (Sternberg and Bardow, 2016), methanol (Daggash et al., 2018) and ammonia (Wang et al., 2017). These chemicals have different properties in terms of energy density, state of aggregation, etc. (Wang et al., 2020). The environmental performance of the corresponding power-to-fuels processes has also been analyzed using life cycle assessment tools, for instance, for methane (Blanco et al., 2020) or methanol (Al-Qahtani et al., 2020).

These fuels have also been proposed as energy carriers for heating and transportation applications (Stančin et al., 2020). Hydrogen and methane were evaluated for heating uses in the on-going project by Thema et al. (2019). Different fuels are also attracting attention for transportation such as ammonia through different conversion technologies (Giddey et al., 2017) or methanol for overseas energy transport (Al-Breiki and Bicer, 2020).

Some important considerations have to be made in order to make use of these fuels as energy carriers or in storage applications. First, the location of the production site plays a key role as wind and solar availability is highly distributed. In addition, as there are fluctuations in the power generation from solar and wind on an hourly scale, the chemical production processes have to be designed with such dynamics in mind. Zhang et al. (2019a) developed an integrated design framework for process networks that produce fuels and power from solar, wind and biomass. Their analysis shows that reasonable plant designs can only be obtained if detailed operational constraints are taken into account in the design optimization problem. Demirhan et al. (2020) assessed the benefit of producing fuels from electricity at one location and transporting them to another location to serve its energy demand. In their particular case study, they considered the states of Texas and New York, respectively. Other existing works focus on supply chain optimization but do not consider details in the operation of the power-to-fuels processes. Seo et al. (2020) considered hydrogen supply chain optimization in which hydrogen from different productions sites is consolidated into an integrated bulk storage to satisfy the demand of electric vehicles. Several energy sources were analyzed, including natural gas, biomass, wind and solar. Ehrenstein et al. (2020) determined the optimal hydrogen supply chain in the UK, but the intermittent nature of solar and wind is only considered through a capacity factor. Ogumerem et al. (2019) considered hydrogen, ammonia and methanol in a multi-period supply chain optimization problem for different states in the US. Here, the length of each time period was set to one year.

In this work, the synthesis of different fuels as a way to store and distribute solar/wind energy is evaluated. With sufficient fuel inventory, it is possible to ensure a stable energy supply with intermittent solar/wind availability. This is especially important in the current context where the energy system must be adapted to achieve climate neutrality. Two levels of decision-making are considered in this work in an integrated approach: network design at the supply chain level and design and operation of the facilities at the scheduling level. At the supply chain level, the production and storage sites are determined as well as the transportation network to distribute the fuels. At the scheduling level, the detailed operation of the facilities and the impact of the intermittent resource availability is analyzed.

2. Problem statement

The goal of this work is to determine the optimal infrastructure to transform intermittent renewable energy (wind and solar) into chemicals that can then be used as energy storage or carrier in different energy applications. A geographical region that is divided in a set of subregions is considered, with given information about solar and wind availability, CO_2 emissions and energy consumption. The objective is to meet a given energy demand in each of the locations using the chemical storage while minimizing the capital and operating costs of the network. To transport the chemicals between the different regions, there are different alternatives: rail, truck and natural gas pipeline. These transportation options are limited by the current infrastructure.

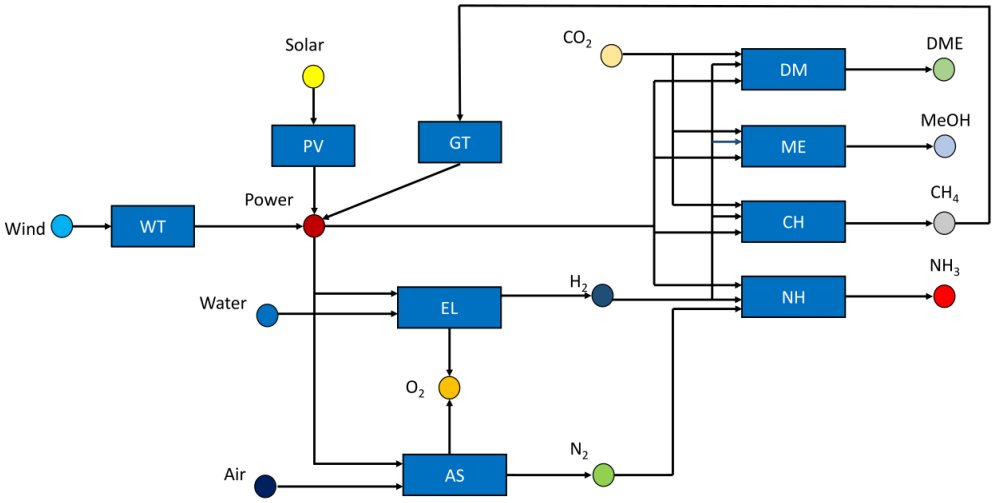

Figure 1: Process-resource network superstructure for the conversion of wind/solar energy to chemicals where rectangles are process nodes and circles are resources nodes.

For chemical storage of renewable energy, the superstructure proposed in Figure 1 is considered. It is represented as a network of processes and resources, similar to an Resource-Task Network (RTN) commonly used in production scheduling (Castro et al., 2004). The circles represent the resources involved in this power-to-fuels system and the rectangles the processes. Four chemicals are considered as energy carriers in this work: methane, methanol, dimethyl ether (DME) and ammonia. To synthesize these chemicals, power is collected from PV panels and/or wind turbines. This energy is used to split water generating hydrogen and to separate air to produce nitrogen. The three first chemicals are synthesized combining hydrogen with CO_2. This CO_2 is obtained using

carbon capture. Ammonia can be produced using nitrogen and hydrogen. Power from methane can be generated using a gas turbine. As a summary, the list of the processes can be found in Table 1.

Intermittency is the main challenge in the operation of chemical plants using renewable energy. It requires a paradigm shift from the traditional steady-state process operation in the chemical industry. Therefore, operation over the course of a year is considered in this work, and hourly time discretization is incorporated in order to capture short-term variations in solar and wind resources. In the optimization problem, the capacities of the production processes, the storage capacities and their locations are determined, as well as the fuel distribution connections between different subregions. Additionally, for each time period, the production rate, the storage amount, the operating mode and the transportation of the different chemicals are calculated.

Table 1: Process description with the input/output resources

Name	Description	Input Resources	Output Resources	Reference
WT	Wind turbines	Wind	Power	de la Cruz and Martín (2016)
PV	Photovoltaic panels	Solar	Power	Sánchez and Martín (2018a)
EL	Water electrolysis	Water, Power	Hydrogen, Oxygen	Sánchez and Martín (2018a)
AS	Air separation unit (distillation, membrane, PSA)	Air, Power	Nitrogen, Oxygen	Sánchez and Martín (2018b)
DM	DME production	Hydrogen , CO_2, Power	DME	Martín (2016b)
ME	Methanol production	Hydrogen, CO_2, Power	Methanol	Martín (2016a)
CH	Methane production	Hydrogen , CO_2, Power	Methane	Davis and Martín (2014)
NH	Ammonia production	Nitrogren, Hydrogen, Power	Ammonia	Sánchez and Martín (2018a)
GT	Gas turbine	Methane	Power	León and Martín (2016)

3. Model formulation

In this section, an integrated supply chain and scheduling model that optimizes the fuels production using wind/solar energy, the location of these plants and the distribution of the fuels to given demand points is presented. The model is based on previous works by Zhang et al. (2016) and Zhang et al. (2019a).

3.1. Process analysis

The processes involved in the power-to-fuels network have been analyzed in previous works (see Table 1). The preceding analyses determined the optimal operating conditions for the different process units and provided the optimal yield for each one of them. The process design evaluation also includes the cost analysis providing the capital and operating cost of each unit of the superstructure presented in Figure 1. In solar PV panels and wind turbines, solar irradiance and wind velocity are used to compute the power production. An efficiency of 25% and a performance ratio of 75 % are assumed for PV panels. A Nordex N100-2500 type wind turbine is selected with a nominal power of 2,500 kW. Davis and Martín (2014) studied the synthesis of methane using hydrogen from water electrolysis powered by renewable energy and CO_2. The synthesis of DME (Martín, 2016b) and methanol (Martín, 2016a) using these same resources have also been analyzed. Sánchez and Martín (2018b) optimized the synthesis of ammonia using air and water. Three different air separation units were evaluated: membrane, pressure swing adsorption and cryogenic distillation. These three alternatives to produce nitrogen were used, mainly, depending of the production scale, and are represented by the AS process in the proposed superstructure. For each of these processes, represented as a rectangle in Figure 1, linear yields have been calculated at the optimal conditions obtained in each of the previous works.

3.2. Time representation

In this work, a multiscale time representation is applied. The time horizon is divided into seasons, denoted by index h. The seasons do not necessarily have to match the four seasons of the year. Each season can have different lengths according to the recurring patterns presented in some of the input resources (solar, wind, etc.). Each season is described by a set of time periods with length Δt. A cyclic schedule, captured using the specified set of time periods, is applied n_h times in each season h. The time periods of each season start at time point 0. The time periods before 0 are only used to impose constraints on the mode transitions. Although a cyclic schedule is imposed in each season, inventory can be carried over from one season to the next, allowing the seasonal storage of chemical fuels, which is an important feature of this model.

3.3. Mass balance constraints for each location

The general process mass balance for each of the locations in the selected geographical region is as follows:

$$\overline{Q}_{rjht} = \overline{Q}_{rjht-1} + B_{rjht} - S_{rjht} + \sum_i \rho_{ij} P_{riht} + \sum_{r' \in \hat{R}_{jr}} W_{jr'rht} - \sum_{r' \in \hat{R}_{jr}} W_{jrr'ht} \quad \forall\, r, j, h, t \in \overline{T}_h \tag{1}$$

with $\hat{R}_{jr}$ being the set of locations to which resource j can be distributed from location r. Five main contributions are involved in equation (1): storage, input and output resource at the selected location, production and transportation to other locations. The amount of resource j stored at location r at time t of season h is represented by $\overline{Q}_{rjht}$. The amounts of consumed or discharged resource at each location are denoted by B_{rjht} and S_{rjht}. The amount of reference resource produced or consumed is denoted by P_{riht}. The parameter ρ_{ij} denotes the conversion factor between resource j and the reference resource of process i. Finally, $W_{jrr'ht}$ is the amount of resource j transported from location r to location r'.

The production of the reference resource in each process i is limited by the plant capacity:

$$P_{riht} = \eta_{riht} C_{ri} \quad \forall\, r, i \in \{PV, WT\}, h, t \in \overline{T}_h \tag{2}$$

$$P_{riht} \leq \eta_{riht} C_{ri} \quad \forall\, r, i \in I \setminus \{PV, WT\}, h, t \in \overline{T}_h \tag{3}$$

The plant capacity is denoted by C_{ri}. The parameter η_{rikt} is used to represent the time-varying process capacity, for instance, wind or solar generation, where the capacity is not only a function of the plant size but also of the wind/solar availability. This parameter is calculated using the solar irradiance or the wind velocity for each time period and location.

The storage capacity $\overline{C}_{rj}$ is an upper bound for the inventory level.

$$\overline{Q}_{rjht} \leq \overline{C}_{rj} \quad \forall\, r, j \in \hat{S}, k, t \in \overline{T}_h \tag{4}$$

$$\overline{Q}_{rjht} = 0 \quad \forall\, r, j \notin \hat{S}, k, t \in \overline{T}_h \tag{5}$$

The set $\hat{S}$ consists of all resources that can be stored (hydrogen, DME, methane, methanol and ammonia).

There is a maximum value for the capacity for each process involved in the network. The binary variable x_{ri} indicates whether process i is selected in the process network at

location r. The maximum allowed process capacity is denoted by $C_i^{\max}$.

$$C_{ri} \leq C_i^{\max} x_{ri} \quad \forall\, r,\, i \tag{6}$$

Similarly, there is also a maximum value for the storage capacity denoted by $\overline{C}_j^{\max}$. The binary variable $\bar{x}_{rj}$ is equal to 1 if a storage facility for product j is built at location r.

$$\overline{C}_{rj} \leq \overline{C}_j^{\max} \bar{x}_{rj} \quad \forall\, r,\, j \tag{7}$$

The resource availability is also limited for those resources used as raw materials in the system (indicated by the set $\hat{B}$).

$$B_{rjht} \leq B_{rjht}^{\max} \quad \forall\, r,\, j \in \hat{B},\, h,\, t \in \overline{T}_h \tag{8}$$

$$B_{rjht} = 0 \quad \forall\, r,\, j \notin \hat{B},\, h,\, t \in \overline{T}_h \tag{9}$$

Some resources do not have an associated demand (i.e., they are not in the set $\hat{J}$). Therefore, the outlet flowrate of these species is fixed to 0:

$$S_{rjht} = 0 \quad \forall\, r,\, j \notin \hat{J},\, h,\, t \in \overline{T}_h \tag{10}$$

3.4. Transportation constraints

To reduce the size of the problem, only transportation connections between neighboring subregions are considered. Three different modes of transportation are contemplated in this study: truck, rail and pipeline. Truck connections are available for all the subregions but rail and pipeline are limited according to the current infrastructure in the region.

The amount of resource j transported from location r to location r' is the summation of the amounts transported using the different transportation modes:

$$W_{jrr'ht} = \sum_{d \in \hat{N}_{jrr'}} T_{jrr'dht} \quad \forall\, j,\, r,\, r',\, h,\, t \in \overline{T}_h \tag{11}$$

The variable $T_{jrr'dht}$ represents the amount of resource j transported from location r to r' using the mode of transportation d. The set of transportation options that can be selected for shipping resource j from location r to r' according to the limitation in the current infrastructure is denoted by $\hat{N}_{jrr'}$.

3.5. Mode-based operation

Each of the processes can operate in four different operating modes: off, startup, on and shutdown. The binary variable y_{rimht} indicates if a process i is operating in a

certain mode m. If a process is selected, one of the operating modes must be assigned:

$$\sum_{m \in M_{ri}} y_{rimht} = x_{ri} \quad \forall\, r,\, i,\, h,\, t \in \overline{T}_h \tag{12}$$

The set M_{ri} denotes the set of allowed operating modes for process i at location r.

The amount of reference resource consumed or produced by process i, P_{riht}, must be produced or consumed in one of the different operating modes. The variable $\overline{P}_{rimht}$ denotes the quantity of reference resource consumed or produced in mode m:

$$P_{riht} = \sum_{m \in M_{ri}} \overline{P}_{rimht} \quad \forall\, r,\, i,\, h,\, t \in \overline{T}_h \tag{13}$$

A maximum ($\widetilde{C}^{\max}_{rim}$) and minimum ($\widetilde{C}^{\min}_{rim}$) value for the amount of reference resource produced or consumed for each mode is introduced:

$$\widetilde{C}^{\min}_{rim}\, y_{rimht} \le \overline{P}_{rimht} \le \widetilde{C}^{\max}_{rim}\, y_{rimht} \quad \forall\, r,\, i,\, m \in M_{ri},\, h,\, t \in \overline{T}_h \tag{14}$$

The following constraints are related to the transition between operating modes for the same process unit. The maximum rate of change within a mode is limited by an upper bound ($\bar{\Delta}^{\max}_{rim}$):

$$\begin{aligned} -\bar{\Delta}^{\max}_{rim} - \overline{M}(2 - y_{rimht} - y_{rimh,t-1}) &\le \overline{P}_{rimht} - \overline{P}_{rimh,t-1} \\ &\le \bar{\Delta}^{\max}_{rim} + \overline{M}(2 - y_{rimht} - y_{rimh,t-1}) \quad \forall\, r,\, i,\, m \in M_{ri},\, h,\, t \in \overline{T}_h \end{aligned} \tag{15}$$

The binary variable $z_{rim'mht}$ is introduced to indicate that process i switches from mode m to mode m' at time t. The possible transitions are defined by the following equation:

$$\begin{aligned} \sum_{m' \in \overline{TR}_{rim}} z_{rim'mh,t-1} - \sum_{m' \in \widehat{TR}_{rim}} z_{rimm'h,t-1} &= y_{rimht} - y_{rimh,t-1} \\ \forall\, r,\, i,\, m \in M_{ri},\, h,\, t \in \overline{T}_h & \end{aligned} \tag{16}$$

where the set TR_{ri} includes all the possible mode-to-mode transitions for the process i at location r, and $\overline{TR}_{rim} = \{m' : (m', m) \in TR_{ri}\}$ and $\widehat{TR}_{rim} = \{m' : (m, m') \in TR_{ri}\}$.

A process i must remain for a certain minimum number of time periods ($\theta_{imm'}$) in an operating mode m before switching to another mode m':

$$y_{rim'ht} \ge \sum_{k=1}^{\theta_{imm'}} z_{rimm'h,t-k} \quad \forall\, r,\, i,\, (m, m') \in TR_i,\, h,\, t \in \overline{T}_h \tag{17}$$

Finally, predefined sequences of modes (from mode m to mode m' to mode m'') for a process i can be defined, establishing a fixed stay time for each of the modes involved in the sequence.

$$z_{rimm'h,t-\bar{\theta}_{imm'm''}} = z_{rim'm''ht} \quad \forall\, r,\, i,\, (m,m',m'') \in SQ_i,\, h,\, t \in \overline{T}_h \tag{18}$$

The set SQ_i denotes the set of predefined sequences for process i and $\bar{\theta}_{imm'm''}$ is the fixed stay time in mode m' in the predefined sequence.

3.6. Continuity constraints

Continuity constraints ensure the feasible transition between seasons. A cyclic schedule is imposed; therefore, the initial mode of a season must be the same as the final one.

$$y_{rimh,0} = y_{rimh,|\overline{T}_h|} \quad \forall\, r,\, i,\, m \in M_{ri},\, h \tag{19}$$

$$z_{rimm'ht} = z_{rimm'h,t+|\overline{T}_h|} \quad \forall\, r,\, i,\, (m,m') \in TR_i,\, h,\, -\theta_i^{\max}+1 \le t \le -1 \tag{20}$$

For the transitions between seasons, the state at the final time of one season and at the initial time of the next season must be the same.

$$y_{rimh,|\overline{T}_h|} = y_{rim,h+1,0} \quad \forall\, r,\, i,\, m \in M_{ri},\, h \in H \setminus |H| \tag{21}$$

$$\begin{aligned} &z_{rimm'h,t+|\overline{T}_h|} = z_{rimm',h+1,t} \\ &\forall\, r,\, i,\, (m,m') \in TR_i,\, h \in H \setminus |H|,\, -\theta_i^{\max}+1 \le t \le -1. \end{aligned} \tag{22}$$

The storage of chemicals is allowed between seasons since that is the key of using fuels for seasonal storage. The following equations determine the change in inventory levels from one season to the next.

$$\hat{Q}_{rjh} = \overline{Q}_{rjh,|\overline{T}_h|} - \overline{Q}_{rjh,0} \quad \forall\, r,\, j \in \hat{S},\, h \tag{23}$$

$$\overline{Q}_{rjh,0} + n_h\, \hat{Q}_{rjh} = \overline{Q}_{j,h+1,0} \quad \forall\, j,\, h \in H \setminus |H| \tag{24}$$

$$\overline{Q}_{rj,|H|,0} + n_{|H|}\, \hat{Q}_{rj,|H|} = \overline{Q}_{rj,1,0} \quad \forall\, j \tag{25}$$

3.7. Objective function

The objective of this work is to meet a given energy demand $D_{r,power,h,t}$ using chemical fuels. The fuels' heating values (H_j) and their average efficiencies (ν_j) are used to

compute the amount of energy that can be produced from them.

$$\sum_{j \in \hat{J}} S_{rjht} H_j \nu_j \geq D_{r,power,h,t} \quad \forall\, r,\, h,\, t \in \overline{T}_h \tag{26}$$

The goal is to minimize the following objective function:

$$\begin{aligned} OP = & \sum_i \sum_{m \in M_{ri}} \sum_r \sum_h \sum_t J_{rimht} + \sum_i \sum_m \sum_r \sigma_i \left(\delta_i x_{ri} + \gamma_i C_{ri}\right) + \\ & \sum_{j \in \hat{S}} \sum_r \left(\alpha_j \bar{x}_{rj} + \beta_j \overline{C}_{rj}\right) + \sum_j \sum_r \sum_{r'} \sum_m \sum_h \sum_t \left(T_{jrr'dht} \Gamma_{jd} \Upsilon_{rr'}\right) \\ & + \sum_r \sum_h \sum_t \varphi_{CO_2} B_{r,CO_2,ht} \end{aligned} \tag{27}$$

which comprises the costs of production, storage and transportation. To estimate the production costs associated with the different processes, the methodology proposed by Sinnott (2005) is used. Two terms contribute to this cost for each process. The variable J_{rimht} is the operating cost of process i in mode m in time period t at location r. This term is calculated through a piece-wise linear approximation. The second term represents the part of the production cost related to the capital investment. A linear capital cost for each of the processes is assumed in this work. The linearization of the different capital costs of each of the procceses has been obtained from previous works (see Table 1). The cost associated with storage is represented by the third term of equation (27). It is assumed that the main contributor to this cost is the amortization of the capital cost for the storage facilities. A linear investment cost for the storage sites is assumed. The operating cost for storage is neglected as it is only a very small fraction of the total storage cost in the case of the considered chemical fuels (Connolly et al., 2016). The next term includes the transportation cost. The parameter Γ_{jd} denotes the shipment cost for resource j in the transportation mode d and $\Upsilon_{rr'}$ the distance between locations r and r'. Finally, to include the cost of CO_2 capture, a CO_2 price is included (φ_{CO_2}) in the objective function.

The piece-wise linear approximation used to compute the first term of equation (27), J_{rimht}, is as follows:

$$P_{rimht} = \sum_{l \in L_i} \left(\lambda_{rimhtl} \left(\hat{P}_{im,l-1} - \hat{P}_{im,l}\right) + \hat{P}_{iml} \omega_{rimhtl}\right) \quad \forall\, r,\, i,\, m \in M_{ri},\, h,\, t \tag{28}$$

$$J_{rimht} = \sum_{l \in L_i} \left(\lambda_{rimhtl} \left(\hat{J}_{im,l-1} - \hat{J}_{im,l}\right) + \hat{J}_{iml} \omega_{rimhtl}\right) \quad \forall\, r,\, i,\, m \in M_{ri},\, h,\, t \tag{29}$$

$$\lambda_{rimhtl} \leq \omega_{rimhtl} \quad \forall\, r,\, i,\, m \in M_{ri},\, h,\, t,\, l \in L_i \tag{30}$$

$$\sum_{l \in L_i} \omega_{iktl} = y_{ikt} \quad \forall\, r,\, i,\, m \in M_{ri},\, h,\, t \tag{31}$$

The optimization problem resulting from equations (1)-(31) is a mixed-integer linear program (MILP). All models used in this work were implemented in Julia using the JuMP package (Lubin and Dunning, 2015). The MILP problems were solved using CPLEX 12.8 with an optimality gap of 1%.

4. Heuristic Decomposition

If the proposed integrated model from Section 3 is solved as such, a large computational time is required, if tractable at all. Hence, a heuristic decomposition approach was considered to address the integrated supply chain and scheduling problem. The first step is to solve the supply chain problem using an aggregated production model. This multiperiod supply chain problem only includes a monthly time discretization; therefore, only average values of wind velocity or solar irradiance can be considered for each month. After solving this problem, the following results are extracted: the locations of the different production and storage facilities, the types of fuels to be produced and the transportation network including the mode of transportation used to meet the energy demand in each of the subregions.

In the second step, a detailed scheduling problem is solved for each of the production facilities to be built. The processes and storage alternatives (but not their capacities) selected in the supply chain optimization step are fixed in the scheduling problem. The demand of the different fuels is also fixed according to the supply chain results. Gas turbine and methane production can further be selected in the scheduling step in order to guarantee a minimum level of production in the chemical process units if no wind and solar sources are available. At the scheduling level, the production and storage capacities for the different production plants are optimized and the operating schedules for the installed facilities are determined.

To get a sense of the effectiveness of this heuristic decomposition approach, a small problem is solved which allows a comparison between the results from solving the full size model and those obtained from the heuristic decomposition. Three locations and a time horizon of one month are selected (more details of this case study can be found in the Supplementary Information). The transport of chemicals is allowed only one time per month in the case of using train or truck, but continuous distribution is possible if a pipeline is used to transport the methane. First, the full integrated supply chain and scheduling problem is evaluated. This integrated model has approximately 1,065,000 variables and 621,000 constraints and was solved in about 150,000 s. Only one production facility is set up at location 1. In terms of the chemicals produced to meet the energy demand, only methane is selected. From location 1, methane is distributed to the other two locations. A combination of solar and wind is selected to capture the

power required for the chemical production (see Table 2). A gas turbine is also selected to maintain a minimum rate of methane production when no wind or solar are available. Methane and hydrogen storages at the production facility (location 1) are used and methane is stored at locations 2 and 3 since no pipeline connection is available for these three places.

Table 2: Comparison between the integrated model and the heuristic decomposition for the production capacities

	Integrated Model	Heuristic Decomposition	
		Supply Chain Problem (intermediate results)	Scheduling Problem (final results)
Solar	14,374 m^2 ($2 MM)	0 m^2 ($0 MM)	14,377 m^2 ($2 MM)
Wind	17,789 m^2 ($9 MM)	4,998 m^2 ($3 MM)	17,793 m^2 ($10 MM)
Eletrolyser	8,504 kW ($36 MM)	1,897 kW ($23 MM)	8,506 kW ($36 MM)
Methane	24 kW ($0.8 MM)	8 kW ($0.5 MM)	24 kW ($0.8 MM)
Gas Turbine	12 kW ($0.1 MM)	0 kW ($0 MM)	13 kW ($0.1 MM)

This problem is also solved using the proposed heuristic decomposition. Firstly, the supply chain problem is solved. The problem has around 950 variables and 720 equalities/inequalities and the solution time is less than 1 second. At this level, the location of the production facilities is determined with only one plant located at location 1 (as in the integrated problem). Only methane is produced and distributed among the locations. The amount of methane that must be transported is also determined at this step. In Table 2, the production capacities obtained solving the supply chain problem are included. These are only internal results of the heuristic decomposition because the actual values of these capacities are those obtained from the scheduling problem as explained next. For the production facility, located at location 1, the scheduling level is computed. From the supply chain solution, the process is fixed to use an eletrolyser and produce methane. PV panels and wind turbines are included to determine the optimal combination in the scheduling model. Finally, a gas turbine is also selected to maintain a certain level of production if no wind or solar based power is generated. This problem is around 295,000 variables and 194,000 constraints and was solved in approximately 3,001 s. The final production and storage capacities for the facility are obtained from this scheduling problem, see Table 2 for the details. One can observe a significant increase in the production capacities compared to those obtained in the supply chain

problem. The total investment for the facility increases from \$26.5 MM to \$48.9 MM, about 80%. Solar PV panels and the gas turbine are included in the scheduling level regarding the supply chain results. This reflects the paramount importance of including the hourly time discretization in order to calculate the capacities required to handle the fast fluctuations in solar and wind availability.

From these results, one can see that by solving the supply chain problem, appropriate (i.e. optimal or near-optimal for the full problem) discrete decisions related to process selection and location are determined. Then, the scheduling problem determines the required capacities and the optimal operational decisions. Consequently, this heuristic decomposition provides a simple but effective means of obtaining a high-quality solution of the integrated supply chain and scheduling problem. In this particular case, it yields the same results as the original full model while reducing the computational time by more than 99 %.

5. Results and Discussion

In the presented computational case study, a region of Spain, the province of Leon, is considered where coal-based power generation is especially significant, and, therefore, energy transition is particularly urgent. Currently, there are three coal-fired power plants with an installed capacity of about 2,300 MW. These facilities are being decommissioned in 2020 due to the new environmental restrictions imposed by the European Commission. This will have significant economic, environmental, and social impacts on the region. Therefore, an effective transition towards a more sustainable energy system is of utmost and urgent importance.

The objective is to design a supply chain that is able to meet a given fraction of the local energy demand using the chemical fuels presented in Section 2. The total energy consumption in this region is about 17.2 TWh per year and it is distributed among four main items: power (11%), natural gas (13%), LPG (1%), and liquid fuels (75%) (Junta de Castilla y Leon, 2020). The province is divided into 29 subregions (see Figure 2) according to the administrative distribution (Junta de Castilla y Leon, 2017). The solar (ITACYL, 2020; ADRASE, 2020) and wind (ITACYL, 2020; DatosClima, 2020) availability are obtained for each of the locations from public databases. It is assumed that CO_2 is obtained from the different plants with CO_2 emissions, such as sugar factories, cogeneration facilities, paper industry, etc. through a carbon capture process. The cost of CO_2 is set to 50 \$/t (Rubin et al., 2015). Transportation by truck is available from one subregion to all its neighboring subregions. The connection by rail and pipeline are limited according to the installed infrastructure. In Figure 2, all the data about the current infrastructure and CO_2 sources are included with the energy consumption associated

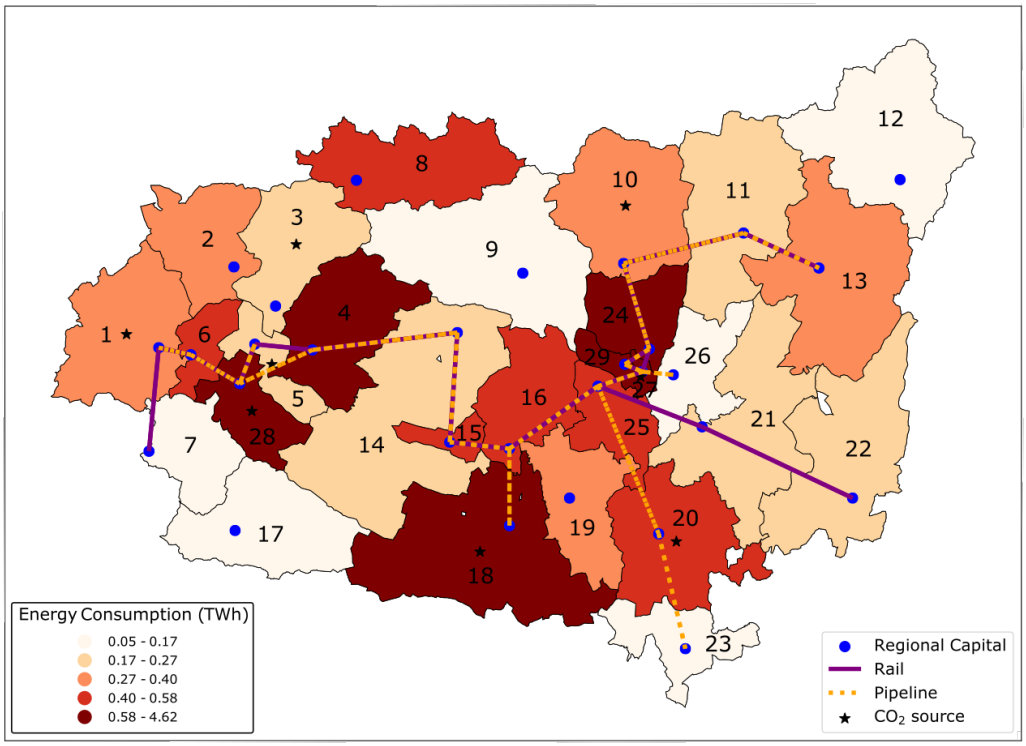

Figure 2: Province of Leon. Energy demand, installed infrastructure and CO_2 sources

with each subregion with different color intensities (Secretaría de Estado de Energía, 2020). The cost of transportation is obtained from different sources for truck (Ministerio de Fomento, 2018), rail (Comisión Nacional de los Mercados y la Competencia, 2017) or pipeline (Saadi et al., 2018).

The maximum area to install PV panels and wind turbines is limited up to 0.5% of the total area of the subregion for each technology, and a maximum utilization of 30% of the total CO_2 emissions is also imposed. A time representation in which the year is divided into 24 seasons, two for each month, with each season represented by a time horizon of a week is applied. For each month, the first corresponding season is the first week of that month in which transportation of chemical fuels using truck or rail is allowed. The second season represents the remaining three weeks of the month in which no distribution via truck and rail is considered.

The heuristic decomposition of Section 4 is applied to solve this problem. The first step is the supply chain level. The size of supply chain problem of this region is about 73,000 variables (18,000 binary variables) and about 110,000 constraints. Considering the total energy consumption of the region, 17.2 TWh, a total energy demand of 1 TWh

has been considered as the maximum level for the fuels. Then, the problem is solved for different levels of this maximum energy demand (25%, 50%, 75% and 100%). Figure 3 shows the locations of the production facilities for the four different energy demand rates and the fuels that are produced in each of the facilities.

When the target is to produce 25% of the total energy demand, only three production plants are built and only carbon-based fuels are used (methane and methanol). However, when the energy demand increases, more fuel production is required and the use of ammonia is introduced in the network. As ammonia is a carbon-free chemical, it can be produced in every subregion. According to the results, ammonia is more expensive to produce than some of the carbon-based fuels, however, it is needed when the availability of CO_2 is limited, which may become an important factor as CO_2 emissions will decrease in the future. As one can see in Figure 3, ammonia represents a high percentage of the chemicals to be synthesized when the energy demand rate increases to 75% or 100%. The areas where carbon-based fuels are synthesized remain almost constant for the high rates of energy demand (75% or 100%).

For further analysis, this work focuses on the case of 50% energy demand. The transportation network for this particular case is shown in Figure 4. The preferred way of transporting methane is via the existing pipeline. This alternative allows a continuous transfer of the product, reducing the storage capital and operating cost, and it is competitive in economic terms. Between the truck and rail connections, the latter is preferred due to the lower operating cost. Therefore, if rail infrastructure is available, this way is selected to distribute the fuels.

The amount of fuels transported is higher during the spring/summer months (for instance, April or July in Figure 4). This is due to the higher production of power during spring/summer months (as it is shown later), therefore the fuel production increases and the amount of products to ship is larger.

The next step is to solve the scheduling problem for the seven selected production facilities. Some of the results are presented here to illustrate the behavior of the production plants. For each plant, the scheduling model has about 3.1 million variables (including 1.9 million binary variables) and 2.1 million constraints. For the sake of brevity, the results for only two of the plants are shown. The first one (located in subregion 27) produces only methane and is located at the center of the province. The second is in the most western subregion (subregion 1) where two fuels are produced, methanol and methane.

First, the facility with only methane production is analyzed. Figure 5 shows the scheduling results of two representative weeks for two different months: July and November. There are three sources of power for the different processes: PV panels,

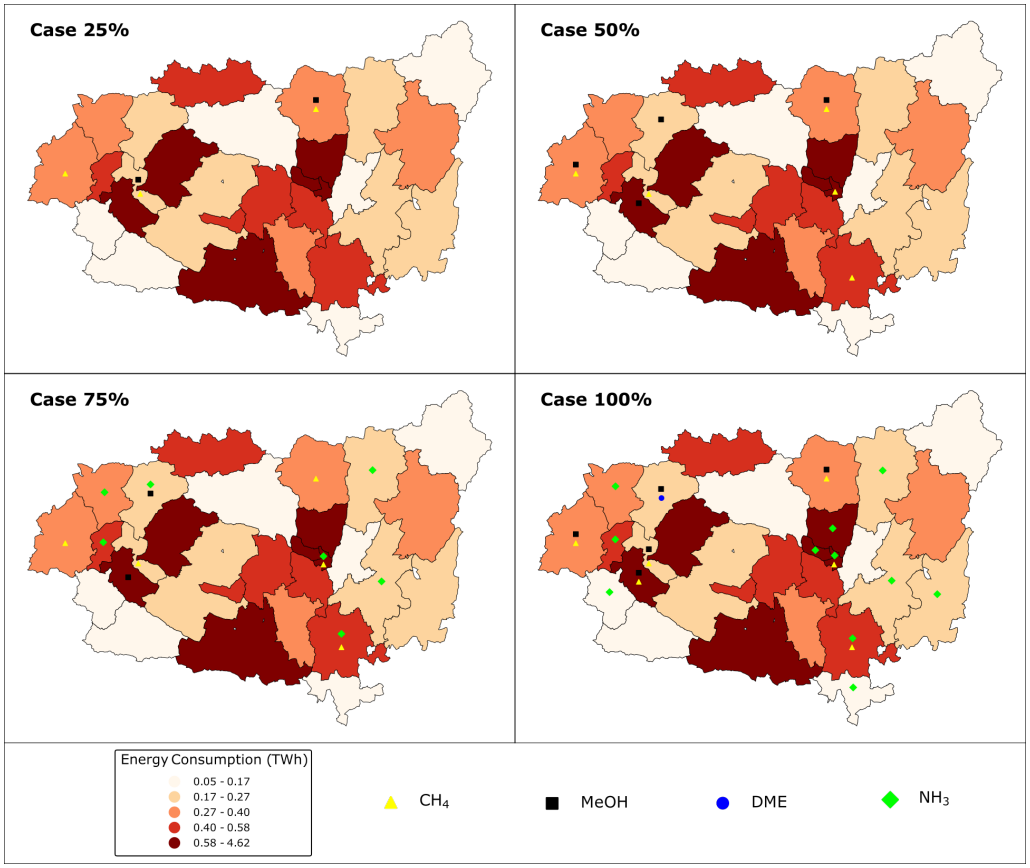

Figure 3: Supply chain results for different rates of the energy demand

wind turbines or gas turbine. The storage level of hydrogen for the different hours is represented by the black line. In July, the power production is higher than in November. During July, more solar-based power generation is produced because the solar irradiance received is larger. In November, solar energy is much lower and wind represents the main power source during this period. The gas turbine only represents a minor fraction of the total power production, reaching zero in some hours. The hydrogen storage is used to mitigate the fluctuations in the renewable based power generation to keep a certain level of production in the chemical manufacturing. In July, hydrogen is stored mainly during the daytime and used at night. The more time-sensitive profile of wind velocity in November results in a different storage schedule for this month.

Figure 6 presents the methane storage level for this facility over the course of the year (red line) and, in gray columns, the power used for the production of methane in each time period. Methane synthesis is more intense during the spring/summer time due to

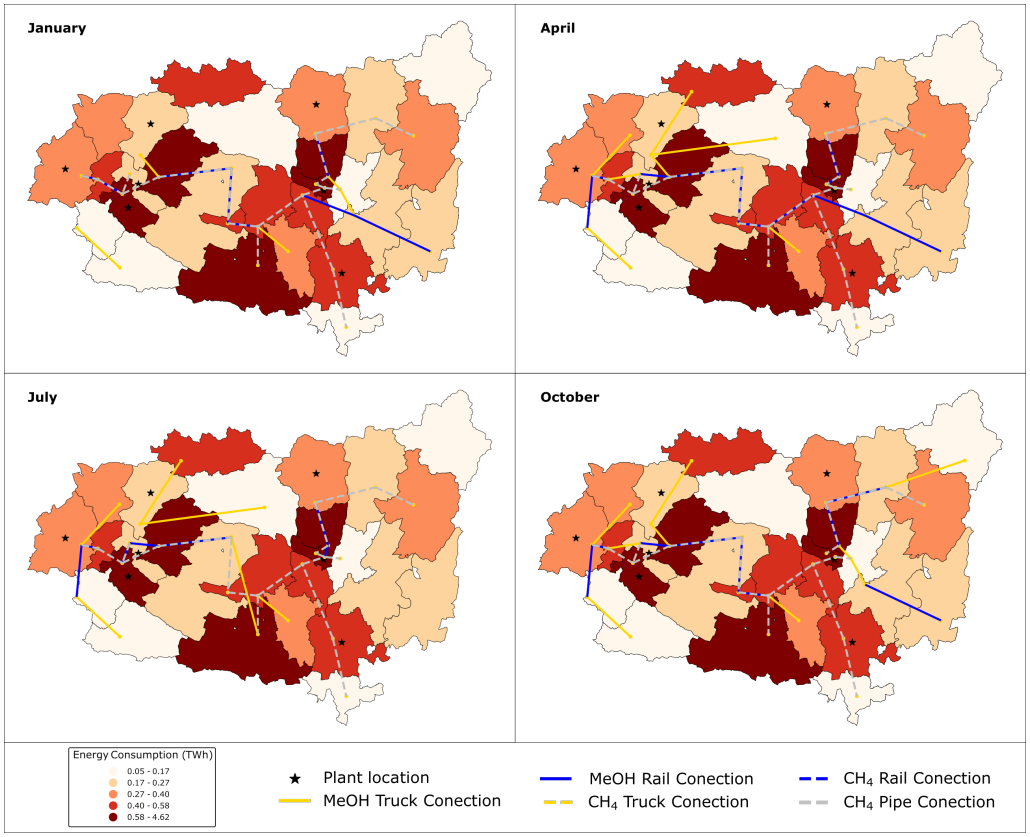

Figure 4: Transportation network for different months of the year

the higher power generation from wind and solar. It is stored during spring/summer reaching the maximum storage level in September/October. Methane is consumed, mainly, during autumn/winter, with the minimum storage in February. It is clear that a significant seasonal storage of the chemical is shown, revealing one of the most important advantages of the use of chemical fuels for energy storage.

The next facility analyzed produces methanol and methane. The scheduling results for a facility where two fuels are synthesized are shown in this section. Firstly, as in the previous case, the power production of two different representative weeks in two particular months is presented (see Figure 7). The results are similar to those obtained in the previous case. Power production is more intense in July than in November. About 250 MW can be produced during some hours of July; however, in November the maximum power production is around 175 MW. Solar is the main source in July, where the longer days translate into higher energy production. Wind has a larger share in November. Different hydrogen storage level profiles are obtained following the availability of

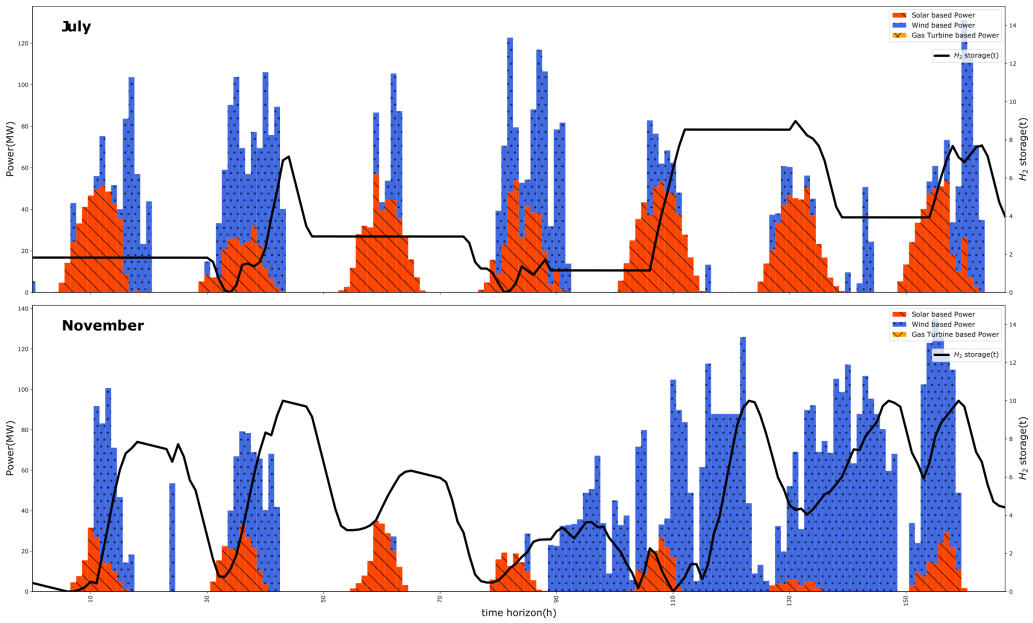

Figure 5: Scheduling results for facility at location one for two different months

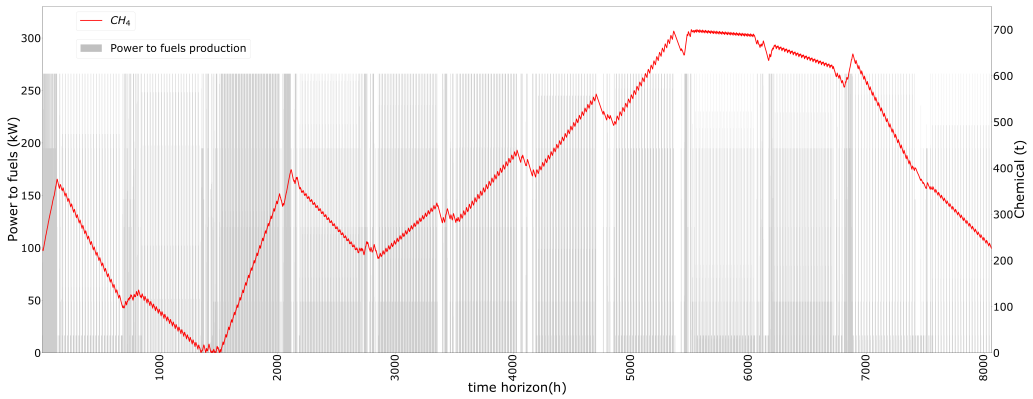

Figure 6: Methane storage/production along the year for facility in subregion 27

solar and wind trying to mitigate their fluctuations.

Figure 8 presents the storage levels for methanol and methane over the course of the year. Power devoted to the production of chemicals is depicted as gray columns. As methanol is a liquid fuel, only rail and truck are available to transport it. Therefore, only one load each month is allowed (at the beginning of the month). During spring/summer time, methanol (blue line) is stored reaching the maximum storage in October/November with about 2,500 t of methanol. The stored methanol is mainly

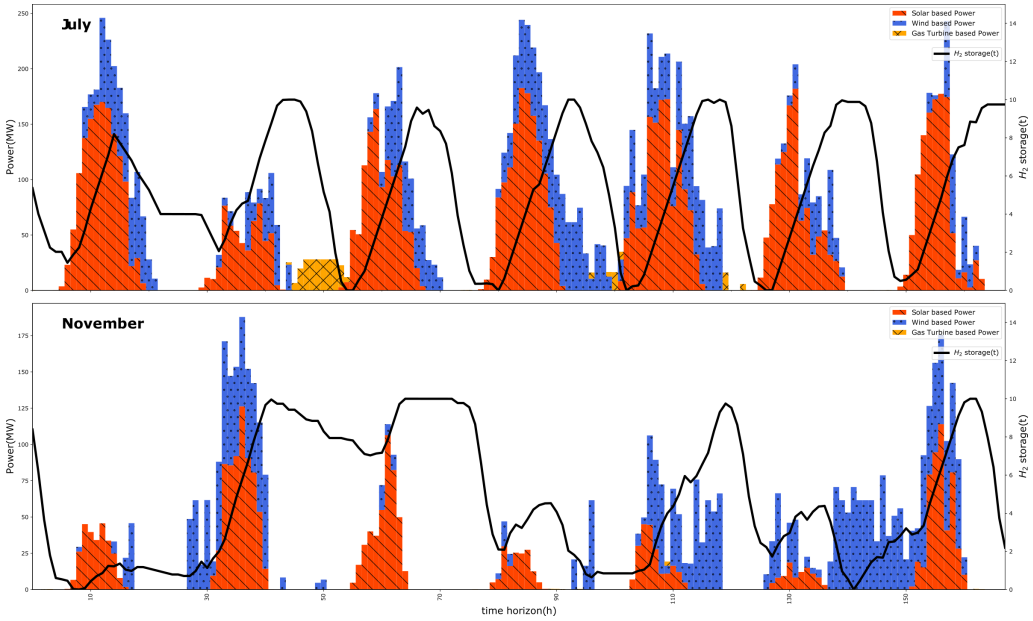

Figure 7: Scheduling results for facility at location three for two different months

used to meet the demand during winter, and the minimum storage level is achieved in February/March. In the case of methane, since can be distributed continuously through pipelines, the storage levels are lower. Storage of a gas such as methane is difficult, therefore, the preferred option for seasonal storage is liquid fuels such as methanol at this location.

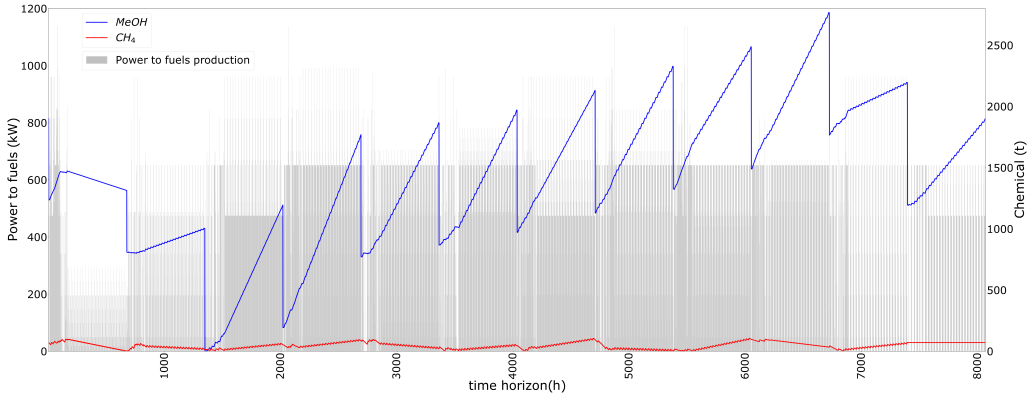

Figure 8: Methanol/Methane storage/production along the year for facility in subregion 1

The design decisions for all facilities built in the network are presented in Table 3. In total, the network requires an investment of $ 2,341 MM, including the production

facilities and the storage sites, and the total production cost of the network is up to $198 MM per year.

Table 3: Production capacities for the facilities in the region of Leon (Spain)

	Plant 1	Plant 3	Plant 5	Plant 10	Plant 20	Plant 27	Plant 28
PV panels (km^2)	0.882	0.365	0.069	1.230	0.115	0.264	1.077
Wind Turbine (number of turbines)	25	11	2	32	5	36	0
Electrolyser (kW)	84,741	35,263	5,424	89,233	11,432	86,779	64,816
DME (kW)	0	0	0	0	0	0	0
CH_4 (kW)	487	5	17	487	25	266	5
MeOH (kW)	651	494	0	1,423	0	0	996
NH_3 (kW)	0	0	0	0	0	0	0
Gas turbine (kW)	28,046	485	6	442	0	0	485

6. Conclusions

In this work, an integrated supply chain and scheduling model has been proposed to determine the optimal power-to-fuels supply network for a given geographical region. A heuristic decomposition method has been developed that achieves high-quality solutions in a reasonable computational time. The proposed decomposition has been validated for a small case study achieving the same results as using the full formulation. The proposed framework has been applied to a region of Spain, where the energy transition is especially significant. The results show that carbon-based fuels such as methane or methanol are preferred when energy demand is low but ammonia is introduced when this demand increases because its production is not limited by the availability of CO_2. Liquid fuels such as methanol or ammonia are used for seasonal storage of energy due to the ease and low cost storage. During spring/summer time more energy is produced and devoted to the manufacturing of fuels that are stored for use during autumn/winter seasons. This work shows the potential of power-to-fuels technologies to provide seasonal energy storage, ultimately enabling higher penetration of renewable energy sources. In particular, these results indicate the significant advantages of power-to-fuels supply chains in addressing changes at multiple temporal scales and serving demands at distributed locations.

Nomenclature

Indices / sets/ subsets

$\hat{B}$	resources use as raw material of the network
$h \in H$	seasons in the multiscale time representation
$i \in I$	processes evaluated in the power to fuel network
$j \in J$	resources involved in the network
$\hat{J}$	product with associated demand
$l \in L$	segments in operating cost piecewise-linear approximations
L_i	segments in piecewise-linear approximation
$m \in M$	operating modes for each of the process
M_{ri}	operating modes for a process
$\hat{N}_{jrr'}$	transportation modes available between two locations
$\hat{R}_{jr}$	location to distribute a product from one site
$\hat{S}$	resources that could be stored
$t \in T$	time periods in the multiscale time representation
$\overline{T}_h$	time periods in season h
$\overline{TR}_{im}$	mode transitions to reach mode m
$\widehat{TR}_{im}$	mode transtions to progress from mode m
TR_i	predefined sequences of mode transitions

Parameters

$B^{\max}_{rjht}$	maximum resource that can be consumed
$C^{\max}_{i}$	maximum production capacity
$\overline{C}^{\max}_{i}$	maximum storage capacity
$\widetilde{C}^{\max}_{im}$	maximum production in a given mode
$\widetilde{C}^{\min}_{im}$	minimum production in a given mode
$D_{r,power,h,t}$	power demand
$\hat{J}_{iml}$	operating cost for piecewise-linear approximation
$\overline{M}$	big-M parameter
n_h	number of repetition of the horizon scheduling for a season
$\hat{P}_{iml}$	production level for piecewise-linear approximation
ρ_{ij}	conversion factor of the different products with respect to the reference resource
η_{riht}	availability of production capacity for wind/solar
$\bar{\Delta}^{\max}_{im}$	maximum rate of change
$\theta_{imm'}$	minimum stay time in a certain mode
$\bar{\theta}_{imm'm''}$	fixed stay time for a predefined sequence

$\theta^{\max}$	stay time in a mode
σ_i	conversion factor between capital and operating cost for a process
δ_i	fixed capital cost coefficient
γ_i	unit capital cost coefficient
α_j	annualized fixed capital cost for storing
β_j	annualized unit capital cost for storing
$\Gamma_{j,d}$	unit cost of transportation
$\Upsilon_{r,r'}$	distance between two locations
Δt	length of one time period
λ_{rimhtl}	coefficient for piecewise-linear approximation
ν_j	average efficiency in the fuel to power transformation

Variables

B_{rjht}	amount of resource consumed
C_{ri}	production capacity for different processes
$\overline{C}_{rj}$	storage capacity for different resources
J_{rimht}	process operating cost not related to capital cost
OP	Operating cost
P_{riht}	amount of reference resource produced
$\overline{P}_{imht}$	reference resource produced in certain mode
$\overline{Q}_{rjht}$	inventory level
$\hat{Q}_{rjh}$	net inventory in a season
S_{rjht}	amount of resource release
$T_{jrr'dht}$	amount of transported resource in the different transportation alternatives
$W_{jrr'ht}$	amount of transported resource
x_{ri}	binary variable to select process units
$\overline{x}_{ri}$	binary variable to select storage units
y_{imht}	binary variable to select a mode for a specific process
$z_{imm'ht}$	binary variable for mode transitions
w_{rimhtl}	binary variable for piecewise-linear aproximation

Acknowledgments

The authors acknowledge the FPU, Spain grant (FPU16/06212) and the mobility grant (EST18/0052) from Government of Spain to A.S., and MINECO, Spain grant DPI2015-67341-C2-1-R.

References

ADRASE, 2020. Acceso a datos de radiación solar de españa, mapa zona península. URL: http://www.adrase.com/.

Ajanovic, A., Hiesl, A., Haas, R., 2020. On the role of storage for electricity in smart energy systems. Energy 200, 117473. URL: http://www.sciencedirect.com/science/article/pii/S0360544220305806, doi:https://doi.org/10.1016/j.energy.2020.117473.

Al-Breiki, M., Bicer, Y., 2020. Technical assessment of liquefied natural gas, ammonia and methanol for overseas energy transport based on energy and exergy analyses. International Journal of Hydrogen Energy 45, 34927–34937. URL: https://www.sciencedirect.com/science/article/pii/S0360319920315858, doi:https://doi.org/10.1016/j.ijhydene.2020.04.181. 4th International HYDROGEN TECHNOLOGIES Congress.

Al-Qahtani, A., González-Garay, A., Bernardi, A., Ángel Galán-Martín, Pozo, C., Dowell, N.M., Chachuat, B., Guillén-Gosálbez, G., 2020. Electricity grid decarbonisation or green methanol fuel? a life-cycle modelling and analysis of todays transportation-power nexus. Applied Energy 265, 114718. URL: http://www.sciencedirect.com/science/article/pii/S0306261920302300, doi:https://doi.org/10.1016/j.apenergy.2020.114718.

Alves, M., Segurado, R., Costa, M., 2020. On the road to 100% renewable energy systems in isolated islands. Energy 198, 117321. URL: http://www.sciencedirect.com/science/article/pii/S036054422030428X, doi:https://doi.org/10.1016/j.energy.2020.117321.

Bartela, L., 2020. A hybrid energy storage system using compressed air and hydrogen as the energy carrier. Energy 196, 117088. URL: http://www.sciencedirect.com/science/article/pii/S036054422030195X, doi:https://doi.org/10.1016/j.energy.2020.117088.

Blanco, H., Codina, V., Laurent, A., Nijs, W., Maréchal, F., Faaij, A., 2020. Life cycle assessment integration into energy system models: An application for power-to-methane in the eu. Applied Energy 259, 114160. URL: http://www.sciencedirect.com/science/article/pii/S0306261919318471, doi:https://doi.org/10.1016/j.apenergy.2019.114160.

BloombergNEF, 2019. New energy outlook 2019. URL: https://about.bnef.com/new-energy-outlook/.

Burre, J., Bongartz, D., Brée, L., Roh, K., Mitsos, A., 2020. Power-to-x: Between electricity storage, e-production, and demand side management. Chemie Ingenieur Technik 92, 74–84. URL: https://onlinelibrary.wiley.com/doi/abs/10.1002/cite.201900102, doi:10.1002/cite.201900102, arXiv:https://onlinelibrary.wiley.com/doi/pdf/10.1002/cite.201900102.

Castro, P.M., Barbosa-Póvoa, A.P., Matos, H.A., Novais, A.Q., 2004. Simple continuous-time formulation for short-term scheduling of batch and continuous processes. Industrial & Engineering Chemistry Research 43, 105–118. URL: https://doi.org/10.1021/ie0302995, doi:10.1021/ie0302995, arXiv:https://doi.org/10.1021/ie0302995.

Comisión Nacional de los Mercados y la Competencia, 2017. Informe sobre los servicios de transprote de mercancías por ferrocarril 2017. URL: https://www.cnmc.es/sites/default/files/2264652_5.pdf.

Connolly, D., Lund, H., Mathiesen, B., 2016. Smart energy europe: The technical and economic impact of one potential 100union. Renewable and Sustainable Energy Reviews 60, 1634–1653. URL: https://www.sciencedirect.com/science/article/pii/S1364032116002331, doi:https://doi.org/10.1016/j.rser.2016.02.025.

de la Cruz, V., Martín, M., 2016. Characterization and optimal site matching of wind turbines: Effects on the economics of synthetic methane production. Journal of Cleaner Production 133, 1302 – 1311. URL:

http://www.sciencedirect.com/science/article/pii/S0959652616306874, doi:https://doi.org/10.1016/j.jclepro.2016.06.019.

Daggash, H.A., Patzschke, C.F., Heuberger, C.F., Zhu, L., Hellgardt, K., Fennell, P.S., Bhave, A.N., Bardow, A., Mac Dowell, N., 2018. Closing the carbon cycle to maximise climate change mitigation: power-to-methanol vs. power-to-direct air capture. Sustainable Energy Fuels 2, 1153–1169. URL: http://dx.doi.org/10.1039/C8SE00061A, doi:10.1039/C8SE00061A.

DatosClima, 2020. Datos de viento para una estación meteorológica. URL: https://datosclima.es/Aemethistorico/Viento.php.

Davis, W., Martín, M., 2014. Optimal year-round operation for methane production from co2 and water using wind and/or solar energy. Journal of Cleaner Production 80, 252 – 261. URL: http://www.sciencedirect.com/science/article/pii/S0959652614005563, doi:https://doi.org/10.1016/j.jclepro.2014.05.077.

Demirhan, C.D., Tso, W.W., Powell, J.B., Heuberger, C.F., Pistikopoulos, E.N., 2020. A multiscale energy systems engineering approach for renewable power generation and storage optimization. Industrial & Engineering Chemistry Research 59, 7706–7721. URL: https://doi.org/10.1021/acs.iecr.0c00436, doi:10.1021/acs.iecr.0c00436, arXiv:https://doi.org/10.1021/acs.iecr.0c00436.

Ehrenstein, M., Ángel Galán-Martín, Tulus, V., Guillén-Gosálbez, G., 2020. Optimising fuel supply chains within planetary boundaries: A case study of hydrogen for road transport in the uk. Applied Energy 276, 115486. URL: http://www.sciencedirect.com/science/article/pii/S0306261920309983, doi:https://doi.org/10.1016/j.apenergy.2020.115486.

García-Olivares, A., Solé, J., Osychenko, O., 2018. Transportation in a 100% renewable energy system. Energy Conversion and Management 158, 266–285. URL: https://www.sciencedirect.com/science/article/pii/S0196890417312050, doi:https://doi.org/10.1016/j.enconman.2017.12.053.

Giddey, S., Badwal, S.P.S., Munnings, C., Dolan, M., 2017. Ammonia as a renewable energy transportation media. ACS Sustainable Chemistry & Engineering 5, 10231–10239. URL: https://doi.org/10.1021/acssuschemeng.7b02219, doi:10.1021/acssuschemeng.7b02219, arXiv:https://doi.org/10.1021/acssuschemeng.7b02219.

Gür, T.M., 2018. Review of electrical energy storage technologies, materials and systems: challenges and prospects for large-scale grid storage. Energy Environ. Sci. 11, 2696–2767. URL: http://dx.doi.org/10.1039/C8EE01419A, doi:10.1039/C8EE01419A.

Heuberger, C.F., Staffell, I., Shah, N., Dowell, N.M., 2017. A systems approach to quantifying the value of power generation and energy storage technologies in future electricity networks. Computers & Chemical Engineering 107, 247 – 256. URL: http://www.sciencedirect.com/science/article/pii/S0098135417302119, doi:https://doi.org/10.1016/j.compchemeng.2017.05.012. in honor of Professor Rafiqul Gani.

ITACYL, 2020. Datos meteorógicos. URL: http://www.itacyl.es/agro-y-geo-tecnologia/agrometeorologia-y-suelos/datos-meteorologicos.

Junta de Castilla y Leon, 2017. La junta aprueba el mapa de unidades básicas de ordenación y servicios del territorio de castilla y león. URL: http://comunicacion.jcyl.es/web/jcyl/Comunicacion/es/Plantilla100Detalle/1281372057192/_/1284703452143/Comunicacion?platform=hootsuite.

Junta de Castilla y Leon, 2020. Estadisticas energéticas de castilla y león. URL: https://energia.jcyl.es/web/es/biblioteca/boletin-estadisticas-energeticas.html.

Larsen, H.H., Petersen, L.S., 2013. DTU international energy report 2013: Energy storage options for future sustainable energy systems. Technical University of Denmark.

León, E., Martín, M., 2016. Optimal production of power in a combined cycle from ma-

nure based biogas. Energy Conversion and Management 114, 89 – 99. URL: http://www.sciencedirect.com/science/article/pii/S0196890416300255, doi:https://doi.org/10.1016/j.enconman.2016.02.002.

Leonard, M.D., Michaelides, E.E., Michaelides, D.N., 2018. Substitution of coal power plants with renewable energy sources – shift of the power demand and energy storage. Energy Conversion and Management 164, 27–35. URL: https://www.sciencedirect.com/science/article/pii/S0196890418302000, doi:https://doi.org/10.1016/j.enconman.2018.02.083.

Lubin, M., Dunning, I., 2015. Computing in operations research using julia. INFORMS Journal on Computing 27, 238–248.

Martín, M., 2016a. Methodology for solar and wind energy chemical storage facilities design under uncertainty: Methanol production from co2 and hydrogen. Computers & Chemical Engineering 92, 43 – 54. URL: http://www.sciencedirect.com/science/article/pii/S0098135416301454, doi:https://doi.org/10.1016/j.compchemeng.2016.05.001.

Martín, M., 2016b. Optimal year-round production of dme from co2 and water using renewable energy. Journal of CO2 Utilization 13, 105 – 113. URL: http://www.sciencedirect.com/science/article/pii/S2212982016300038, doi:https://doi.org/10.1016/j.jcou.2016.01.003.

Mehigan, L., Al Kez, D., Collins, S., Foley, A., Ó'Gallachóir, B., Deane, P., 2020. Renewables in the european power system and the impact on system rotational inertia. Energy 203, 117776. URL: http://www.sciencedirect.com/science/article/pii/S0360544220308835, doi:https://doi.org/10.1016/j.energy.2020.117776.

Ministerio de Fomento, 2018. Obsrvatorio de costes del transporte de mercancías por carretera. URL: http://www.fomento.es/MFOM.CP.Web/handlers/pdfhandler.ashx?idpub=TTW128.

Nejat, P., Jomehzadeh, F., Taheri, M.M., Gohari, M., Abd. Majid, M.Z., 2015. A global review of energy consumption, co2 emissions and policy in the residential sector (with an overview of the top ten co2 emitting countries). Renewable and Sustainable Energy Reviews 43, 843 – 862. URL: http://www.sciencedirect.com/science/article/pii/S1364032114010053, doi:https://doi.org/10.1016/j.rser.2014.11.066.

Ogumerem, G.S., Tso, W.W., Demirhan, C.D., Lee, S.Y., Song, H.E., Pistikopoulos, E.N., 2019. Toward the optimization of hydrogen, ammonia, and methanol supply chains. IFAC-PapersOnLine 52, 844 – 849. URL: http://www.sciencedirect.com/science/article/pii/S2405896319302551, doi:https://doi.org/10.1016/j.ifacol.2019.06.167. 12th IFAC Symposium on Dynamics and Control of Process Systems, including Biosystems DYCOPS 2019.

Rubin, E.S., Davison, J.E., Herzog, H.J., 2015. The cost of co2 capture and storage. International Journal of Greenhouse Gas Control 40, 378–400. URL: https://www.sciencedirect.com/science/article/pii/S1750583615001814, doi:https://doi.org/10.1016/j.ijggc.2015.05.018.

Saadi, F.H., Lewis, N.S., McFarland, E.W., 2018. Relative costs of transporting electrical and chemical energy. Energy Environ. Sci. 11, 469–475. URL: http://dx.doi.org/10.1039/C7EE01987D, doi:10.1039/C7EE01987D.

Secretaría de Estado de Energía, 2020. Estadísticas y balances energéticos: Eléctricas 2016-2018. URL: https://energia.gob.es/balances/Publicaciones/ElectricasAnuales/Paginas/Electricas-Anuales2016-2018.aspx.

Seo, S.K., Yun, D.Y., Lee, C.J., 2020. Design and optimization of a hydrogen supply chain using a centralized storage model. Applied Energy 262, 114452. URL: http://www.sciencedirect.com/science/article/pii/S0306261919321403, doi:https://doi.org/10.1016/j.apenergy.2019.114452.

Sinnott, R., 2005. Chemical Engineering Design: Chemical Engineering Volume 6. Elsevier.

Sánchez, A., Martín, M., 2018a. Optimal renewable production of ammonia from water and air. Journal

of Cleaner Production 178, 325 – 342. URL: http://www.sciencedirect.com/science/article/pii/S0959652617332730, doi:https://doi.org/10.1016/j.jclepro.2017.12.279.

Sánchez, A., Martín, M., 2018b. Scale up and scale down issues of renewable ammonia plants: Towards modular design. Sustainable Production and Consumption 16, 176 – 192. URL: http://www.sciencedirect.com/science/article/pii/S2352550918300812, doi:https://doi.org/10.1016/j.spc.2018.08.001.

Stančin, H., Mikulčić, H., Wang, X., Duić, N., 2020. A review on alternative fuels in future energy system. Renewable and Sustainable Energy Reviews 128, 109927. URL: https://www.sciencedirect.com/science/article/pii/S1364032120302185, doi:https://doi.org/10.1016/j.rser.2020.109927.

Sternberg, A., Bardow, A., 2015. Power-to-what? – environmental assessment of energy storage systems. Energy Environ. Sci. 8, 389–400. URL: http://dx.doi.org/10.1039/C4EE03051F, doi:10.1039/C4EE03051F.

Sternberg, A., Bardow, A., 2016. Life cycle assessment of power-to-gas: Syngas vs methane. ACS Sustainable Chemistry & Engineering 4, 4156–4165. URL: https://doi.org/10.1021/acssuschemeng.6b00644, doi:10.1021/acssuschemeng.6b00644, arXiv:https://doi.org/10.1021/acssuschemeng.6b00644.

Thema, M., Bauer, F., Sterner, M., 2019. Power-to-gas: Electrolysis and methanation status review. Renewable and Sustainable Energy Reviews 112, 775–787. URL: https://www.sciencedirect.com/science/article/pii/S136403211930423X, doi:https://doi.org/10.1016/j.rser.2019.06.030.

Thomaßen, G., Kavvadias, K., Jiménez Navarro, J.P., 2021. The decarbonisation of the eu heating sector through electrification: A parametric analysis. Energy Policy 148, 111929. URL: https://www.sciencedirect.com/science/article/pii/S0301421520306406, doi:https://doi.org/10.1016/j.enpol.2020.111929.

Wang, G., Mitsos, A., Marquardt, W., 2017. Conceptual design of ammonia-based energy storage system: System design and time-invariant performance. AIChE Journal 63, 1620–1637. URL: https://aiche.onlinelibrary.wiley.com/doi/abs/10.1002/aic.15660, doi:10.1002/aic.15660, arXiv:https://aiche.onlinelibrary.wiley.com/doi/pdf/10.1002/aic.15660.

Wang, L., Zhang, Y., Pérez-Fortes, M., Aubin, P., Lin, T.E., Yang, Y., Maréchal, F., Van herle, J., 2020. Reversible solid-oxide cell stack based power-to-x-to-power systems: Comparison of thermodynamic performance. Applied Energy 275, 115330. URL: http://www.sciencedirect.com/science/article/pii/S0306261920308424, doi:https://doi.org/10.1016/j.apenergy.2020.115330.

Zhang, Q., Martín, M., Grossmann, I.E., 2019a. Integrated design and operation of renewables-based fuels and power production networks. Computers & Chemical Engineering 122, 80 – 92. URL: http://www.sciencedirect.com/science/article/pii/S0098135418306525, doi:https://doi.org/10.1016/j.compchemeng.2018.06.018.

Zhang, Q., Sundaramoorthy, A., Grossmann, I.E., Pinto, J.M., 2016. A discrete-time scheduling model for continuous power-intensive process networks with various power contracts. Computers & Chemical Engineering 84, 382 – 393. URL: http://www.sciencedirect.com/science/article/pii/S0098135415003142, doi:https://doi.org/10.1016/j.compchemeng.2015.09.019.

Zhang, Y., Wang, L., Wang, N., Duan, L., Zong, Y., You, S., Maréchal, F., Van herle, J., Yang, Y., 2019b. Balancing wind-power fluctuation via onsite storage under uncertainty: Power-to-hydrogen-to-power versus lithium battery. Renewable and Sustainable Energy Reviews 116, 109465. URL: http://www.sciencedirect.com/science/article/pii/S1364032119306732, doi:https://doi.org/10.1016/j.rser.2019.109465.